FEBS Letters 569 (2004) 224–228 FEBS 28536

The African swine fever virus dynein-binding protein p54 induces infected cell apoptosis

Bruno Hernáez[a], Gema Díaz-Gil[a], Mónica García-Gallo[a], José Ignacio Quetglas[a], Ignacio Rodríguez-Crespo[c], Linda Dixon[b], José M. Escribano[a], Covadonga Alonso[a,*]

[a]*Dpto. Biotecnología, Instituto Nacional de Investigación y Tecnología Agraria y Alimentaria (INIA), Ctra. de la Coruña Km 7, 28040 Madrid, Spain*
[b]*Institute for Animal Health, GU24 ONF, Pirbright, UK*
[c]*Dpto. Bioquímica, Facultad de Químicas, Univ. Complutense, Madrid, Spain*

Received 24 March 2004; revised 25 May 2004; accepted 1 June 2004

Available online 9 June 2004

Edited by Hans-Dieter Klenk

Abstract A specific interaction of ASFV p54 protein with 8 kDa light chain cytoplasmic dynein (DLC8) has been previously characterized and this interaction is critical during virus internalization and transport to factory sites. During early phases of infection, the virus induces the initiation of apoptosis triggering activation of caspase-9 and -3. To analyze the role of the structural protein p54 in apoptosis, transient expression experiments of p54 in Vero cells were carried out which resulted in effector caspase-3 activation and apoptosis. Interestingly, p54 mutants, lacking the 13 aa dynein-binding motif lose caspase activation ability and pro-death function of p54. This is the first reported ASFV protein which induces apoptosis.

Keywords: Apoptosis; Virus–cell interaction; African swine fever virus; Dynein light chain; Bim

1. Introduction

African swine fever virus (ASFV) is a double stranded large DNA virus, the only member of the family Asfarviridae [2], that induces an acute disease of swine characterized by severe immune cell depletion and apoptosis induction in target and immune defense cells [3]. ASFV encodes for apoptosis inhibitor homologs [2], the bcl-2 [4,5], and IAP homologs and an homolog of the apoptosis inhibitor ICP34.5 of herpes simplex [2], but the mechanism by which the virus induces apoptosis is still unclear.

ASFV induction of apoptosis in target cells is triggered in the absence of virus replication and after virus uncoating by an unknown mechanism [6]. Some structural proteins of different virus models have been found to trigger apoptosis in early steps of the infective cycle upon their interactions with the target cell [7–10]. Structural ASFV protein #54 (p54) interaction with light chain cytoplasmic dynein of 8 kDa (DLC8) is required for virus transport upon entry [1]. Previously, we described that p54 interacts with one of the light chains of cytoplasmic dynein, a microtubular-based motor, enabling virus transport along the cytosol [1]. DLC8 or PIN interacts with other molecules of the microtubular complex, links microtubules to other cytoskeletal components and binds to specific cargoes [11,12]. A 13 amino acid (aa) domain of ASFV protein p54 was sufficient for binding to DLC8; a SQT motif within this domain being critical for this binding [1]. Dynein light chain DLC8 has been recently recognized as a frequently used target for a number of polypeptides encoded by different virus models [13].

The aa residues required for the viral p54–DLC8 interaction differ from those present in other DLC8 binding proteins [11,14], but it is similar to the binding domain of the proapoptotic BH3-only protein Bim [1,15]. BH3-only proteins have been recognized as essential initiators of apoptosis [16].

ASFV p54 is a major infection protein, essential for viral replication [17] and has been characterized as a viral attachment protein [18,19]. In this work, we analyzed the role of p54 in caspase activation and viral-induced apoptosis.

2. Materials and methods

2.1. Transfections and caspase activity assays

Viral genes encoding for proteins p30, p54 and p72 were individually inserted into *Xho*I and *Eco*RI sites in mammalian expression vector pEGFP-N1 (Clontech, Palo Alto, CA). pEGFP-N1 and pCMV (Clontech) vectors were used as transfection controls. Vero cells were grown to 40–50% confluence and then transfected with 2 μg DNA/10^6 cells using FUGENE6 (ratio 1:6, Roche, Indianapolis, IN).

Caspase-3 and -9 activities were detected in ASFV infected cells at 0, 6, 12, 24 and 48 h postinfection or 24 h posttransfection in transfected cells. Caspase activities were determined by using Caspase-3 Fluorimetric Assay Kit (Sigma, St Louis, MO) and ApoAlert Caspase-9/6 Fluorescent Assay Kit (Clontech, Palo Alto, CA), respectively, according to the manufacturer's directions. Data obtained were normalized to GFP expression found in each plate at excitation and emission wavelengths of 485 and 535 nm in order to refer results obtained with their respective transfection efficiency. To detect specific caspase-3 activity Ac-DEVD-CHO was used as an inhibitor, at a concentration of 2 μM. For caspase-9, LEHD-CHO was used as an inhibitor, at a concentration of 10 μM.

2.2. Generation of a p54 mutant

A mutant, with a 39-bp deletion in p54 from aa 149 to 161, was created by overlap extension (SOE) PCR procedure. The N-terminal part of p54 (aa 1–148, nucleotides 1–444) was amplified by PCR using

* Corresponding author. Fax: +34-91-3573107.
E-mail address: calonso@inia.es (C. Alonso).

Abbreviations: ASFV, African swine fever virus; p54, ASFV protein #54; DLC8, Light chain cytoplasmic dynein of 8 kDa; aa, amino acids; kDa, kilodaltons; casp., caspase

0014-5793/$22.00
doi:10.1016/j.febslet.2004.06.001

primers 5′GCGCTCGAGATGGATTCTGAATTTTTTCA3′ and 5′AGCCGACATAGGCTCAGTCGGATGAGC3′. The C-terminal part of p54 (aa 162–183, nucleotides 486–549) was amplified by PCR using primers 5′ACTGAGCCTATGTCGGCTATTGAAAAT3′ and 5′CGCGAATTCGCAAGGAGTTTTCTAGGTC3′. The resulting products were combined by SOE-PCR. The resulting cDNA construct was digested with *Xho*I and *Eco*RI and inserted into pEGFP-NI vector.

2.3. Virus infections and immunofluorescence

Vero cells were grown in chamber slides containing approximately 1.5×10^4 cells /chamber (Lab-Tek; Nunc, Roskilde, Denmark), and were mock infected or infected with ASF virus strain BA71V at a multiplicity of infection (MOI) of 1, at time points from 4 to 48 hpi and fixed with acetone:methanol 1:1.

An affinity-purified rabbit antibody against DLC8 (R4058) was supplied by Dr. S. King [11] and was used at a 1:200 dilution. Other antibodies used were mouse monoclonal antibodies, anti-Bim (Calbiochem, La Jolla, CA), anti-GFP (JL-8, Clontech) and anti-β tubulin from Sigma. Monoclonal antibodies against viral p30, p72 and monospecific antiserum against viral protein p54 raised in pigs using *Escherichia coli* expressed protein as immunogen were used. Secondary antibodies used were Alexa 488, Alexa 647, Texas Red and Cy3 conjugated sheep anti-rabbit or goat anti-mouse antibodies (Sigma) or protein A Alexa 488 (Molecular Probes, Eugene, CA). DNA was stained with bisbenzimide Hoechst No. 33342 (Sigma).

Caspase-9 activation was detected using a monoclonal antibody (Santa Cruz Biotechnology, Santa Cruz, CA) that recognizes procaspase and activated caspase-9 after proteolysis and a rabbit antibody anti-activated caspase-3 and anti-rabbit antibody Texas Red (Sigma) were used to detect caspase-3 activation. Apoptosis inducing factor (AIF) was detected with a monoclonal antibody also from Santa Cruz. Mitochondria were labelled with 100 nM chloromethyl-rosamine (CMXRos, MitoTracker, Molecular Probes) for 15 min at 37 °C and then fixed with 3.7% paraformaldehyde. For subsequent staining with other antibodies, cells were permeabilized with ice-cold acetone. Specificity of labelling and absence of signal crossover were established by examination of single labelled control samples. Percentages of colocalization were analyzed in at least 10 high power microscopic fields. Conventional microscopy was carried out in a Leica photomicroscope with a digital camera and digitized images were obtained with Qwin program (Leica Microsystems, Heidelberg, Germany). Confocal microscopy was carried out on a Radiance 2100 MRC1024 system (BioRad, Hercules, CA) mounted on a Nikon Eclipse TE2000 microscope. Statistical analysis of colocalization was performed using Laserpix Lasersharp Processing 3.2 program (BioRad).

2.4. Subcellular fractionation

For velocity sedimentation experiments, Vero cells were mock infected or infected with ASF virus strain BA71V at a MOI of 1. At 4, 6, 12, and 24 hpi cells were washed with PBS, scraped and harvested by centrifugation. The pellets were resuspended in 1 ml of buffer A (30 mM Tris, 20 mM Mes, pH 7.0, 100 mM NaCl, and 0.1% Triton X-100) supplemented with protease inhibitors on ice. Lysis was performed by three cycles of sonication (30 s each) at mid-potency. Final volumes of 5.5 ml were prepared of both 5% and 20% sucrose solution in buffer A and a linear gradient was formed. The lysed cells were loaded on top of the preformed 5–20% sucrose linear gradient in buffer A equilibrated at 4 °C and centrifuged in a SW40 Beckman rotor for 16 h at 4 °C. After centrifugation, 1 ml samples were collected from the bottom of the gradient. Protein precipitation from samples was performed with ice-cold acetone at −20 °C overnight. The samples were then centrifuged and the protein pellets resuspended in 200 μl loading buffer. Equal volumes of each sample were subjected to SDS–PAGE and then analyzed by immunoblot with specific antibodies. Expression of DLC8, Bim and β-tubulin during infection was tested by using cell lysates in RIPA buffer (150 mM NaCl, 1% NP-40, 0.1% SDS and 50 mM Tris, pH 8.0) of uninfected and ASFV infected Vero cells harvested at 2, 4, 6, 8, 12, 24 and 48 hpi. These cell lysates were subjected to SDS–PAGE, blotted and probed with specific antibodies.

3. Results

3.1. Activation of the mitochondrial apoptosis pathway in ASFV infected cells

ASFV infected cells expressing high levels of p54 (Fig. 1A a, d and f) expressed the active form of caspase-3 (Fig. 1A b) and presented the characteristic nuclear morphology of apoptosis, i.e., chromatin condensation, nuclear fragmentation and apoptotic body formation with DNA dyes (Fig. 1A c, e and g). High levels of caspase-3 and -9 activity were found at different postinfection times (Figs. 1B and C), which returned to the basal levels in the presence of their specific caspase inhibitor. Activation of apoptosis cascade results in the cleavage of

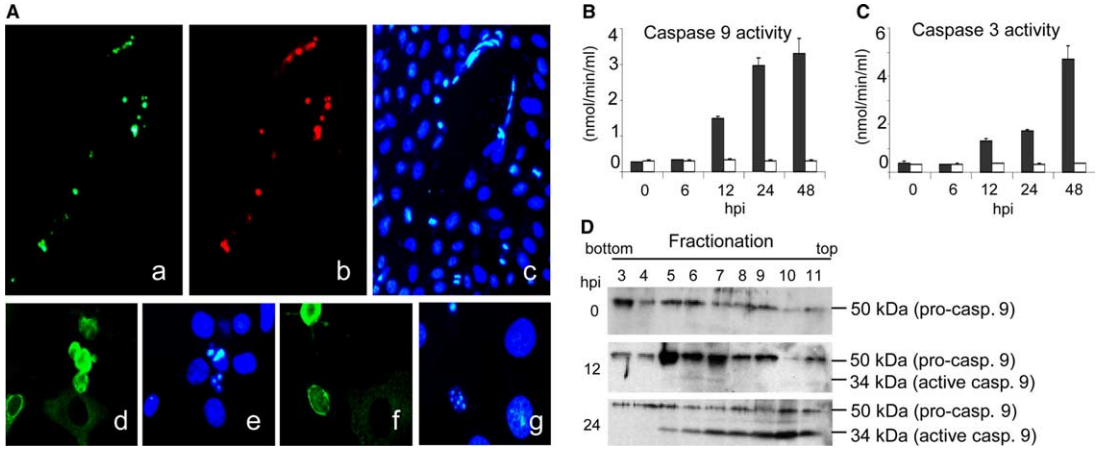

Fig. 1. Caspase activation and nuclear fragmentation after ASFV infection. (A, a–g) ASFV infected Vero cells at 24 hpi stained with anti-ASFVp54 antibody revealed with Alexa 488 (a, d, f), DNA dye Hoechst (c, e, g), and anti-activated caspase-3 and Texas red (b). (A, a–c) Viral lysis plaque (original magnification 100×). (A e, g) Detail of nuclear fragmentation (original magnification, *d* 400×). (B, C) Caspase-3 and -9 activation detected by fluorimetric analysis in cell extracts infected with ASFV. Solid and open bars represent caspase activity in the absence and the presence of a specific caspase inhibitor, respectively, 2 μM Ac-DEVD-CHO was used as caspase-3 inhibitor and 10 μM LEHD-CHO was used as caspase-9 inhibitor. Data obtained were normalized to their respective GFP expression at excitation and emission wavelengths of 485 and 535 nm. The figure shows the mean activities values from three independent experiments ± S.E. (D) Initiator caspase-9 activation was detected since 12 hpi with a monoclonal antibody recognizing pro- and active forms of this protein.

pro-caspases to an active form. Activated caspase-9 was detected, as the processed 32 kDa form (Fig. 1D), indicating activation of the intrinsic or mitochondrial apoptosis pathway.

3.2. ASFV p54 is able to induce apoptosis in infected cells

To elucidate a specific role of p54 in these changes, viral protein p54 was transiently expressed as GFP fusion protein under mammalian promoter CMV. Other viral proteins expressed as GFP fusion proteins, GFP alone and empty plasmid, were used as controls. Plasmids were transfected and yielded high transfection efficiency. P54 transiently expressed in Vero cells, acting without other viral proteins, caused activated caspase-3 expression (Fig. 2A d and e) and nuclear fragmentation (Fig. 2A f), indicating a downstream execution of the apoptotic cell death program. Transient expression of p54 mutant lacking the 13 aa dynein-binding motif did not induce caspase-3 activation or nuclear fragmentation (Fig. 2A g, h and i). Overexpression of other viral proteins p30, p72 (not shown) or GFP alone did not produce apoptosis or caspase activation (Fig. 2A a–c).

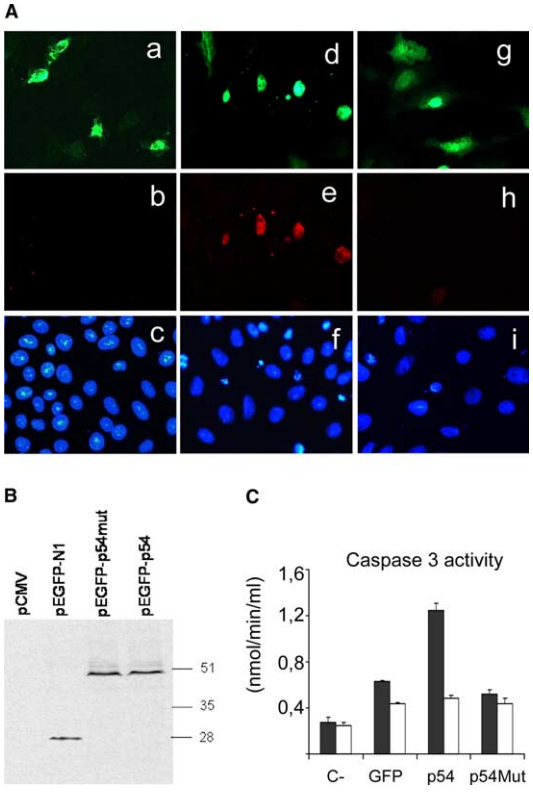

Fig. 2. Caspase-3 activation and apoptosis in p54 transfected cells. (A a, d, g) Green fluorescence protein expression in Vero cells transfected with pCMV-GFP (a–c), pCMVp54-GFP (d–f) and pCMV-mutantp54-GFP (g–i). (b, e, h) Effector caspase-3 expression in the same cells detected with an antibody anti-activated caspase-3 revealed with Texas Red. (c, f, i) Nuclear staining with a DNA intercalating dye by fluorescence microscopy. Original magnification 400×. (B) GFP expression in Vero cells transfected with the different plasmids and detected by Western blot with an anti-GFP antibody. (C) Fluorimetric analysis of caspase activity in Vero cells transfected with pCMV-p54-GFP and pCMV-p54mut-GFP compared with control cells or cells transfected with the control plasmid. Solid bars and open bars show caspase-3 activity in the absence and the presence of the specific caspase inhibitors, respectively, at the same concentrations as in Fig. 1. Data obtained were normalized to the GFP expression found in each plate at excitation and emission wavelengths of 485 and 535 nm.

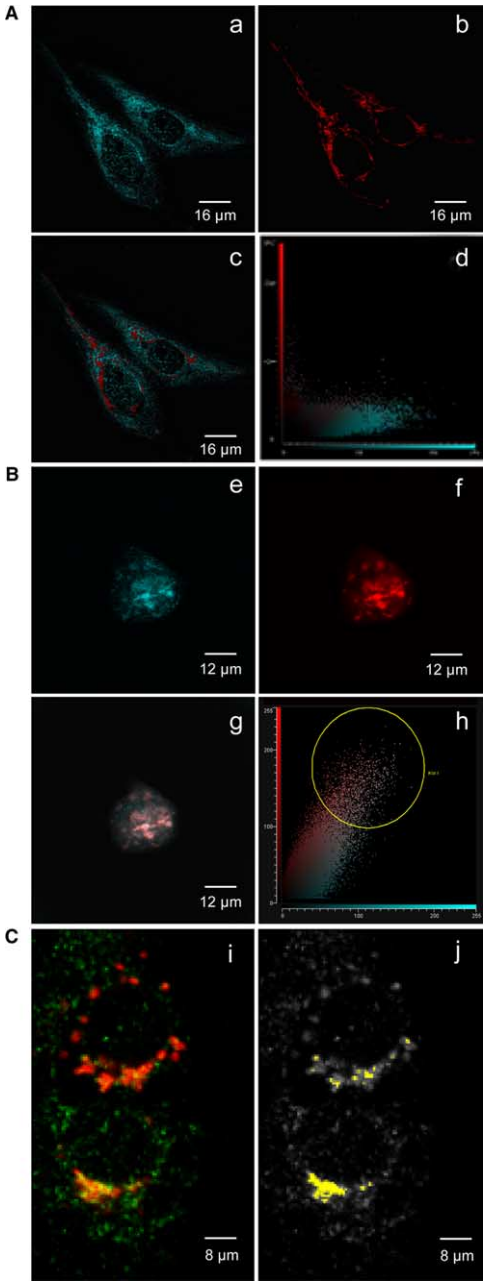

Fig. 3. Bim redistribution to mitochondria in infected cells. Confocal microscopy analysis of Vero cells stained with anti-Bim antibody revealed with Alexa 647 (a, e; depicted in blue) and mitotracker CMXRos (b, f in red) and merged images (c, g) (A) Mock infected Vero cells (B) ASFV infected Vero cells at 24 hpi show Bim colocalization to the clustered mitochondria. (d, h) Dot plot of colocalization probability between Bim and CMXRos. (C) Detail of ASFV infected Vero cells at 18 hpi showing Bim colocalization to mitochondria at higher magnification (bar): (i) Merged image. Bim is shown in green and CMXRos in red. (j) Selection of colocalization areas depicted in yellow.

Expression of GFP was detected with a monoclonal antibody anti-GFP by Western blot as a control of transfection efficiency (over 80% of cells, Fig. 2B). Also, data obtained by fluorimetry were normalized to their respective GFP expression levels at excitation and emission wavelengths of 485 and 535 nm.

Fluorimetric measurement of caspase activity (Fig. 2C) yielded high levels of caspase-3 activity in those cells expressing p54 when compared to controls. Transfection of a plasmid expressing a mutant p54, lacking the 13 aa region including the dynein-binding site, did not produce caspase activation (Fig. 2C) pointing out a role for this region of the protein in ASFV-induced apoptosis.

3.3. Alterations in subcellular localization of proapoptotic protein Bim during ASFV infection

Structural virus protein p54 interacts with dynein by a similar binding sequence than Bim. We investigated Bim subcellular localization after ASFV infection by confocal microscopy analysis. Bim redistribution to mitochondria after infection was detected using an anti-Bim monoclonal antibody and a potential-sensitive dye specific for mitochondria (Fig. 3). In uninfected Vero cells, mitochondria were observed as an almost continuous succession of organelles extending throughout the cytoplasm and Bim showed no colocalization with mitochondria (<2% mean probability) (Fig. 3A). Nevertheless, after ASFV infection, Bim showed colocalization to the clustered mitochondria in discrete spots. From a total of 74% to 82% of infected cells, colocalization was found at 12 hpi over 43% probability, and 89–92% at 24 hpi (Figs. 3B and C). It was accompanied by severe changes in mitochondrial organization during infection of Vero cells (Fig. 3B). Irregular distribution and swelling of mitochondria was visible since 8 h after infection, while at later time points (24 hpi) mitochondria aggregated around the paranuclear location of virus factories close to the microtubular organizing center (MTOC, not shown).

To confirm changes in subcellular localization of Bim during ASFV infection, gel filtration assays were performed. The sedimentation of Bim on sucrose gradients changed, from the heavier fractions, in which microtubule components (β-tubulin) and the associated dynein (DLC8) co-migrated, to upper low density fractions after infection (Fig. 4A). Viral protein p54 was detected in the same fractions. Relocation of Bim occurred within early postinfection times, from 8 to 12 hpi. Bim was found in lower density fractions at 12 hpi. This translocation was accompanied by initiation of downstream apoptotic events and mitochondrial AIF was also detected in lighter fractions of the sucrose gradients at 24 hpi (Fig. 4A) as it exits from the mitochondria. Also caspase-9 and -3 activation (Figs. 1B and C) and alteration of nuclear and mitochondrial morphology were found since 12 hpi (Fig. 1).

To determine if alterations in Bim or DLC8 synthesis occurred along ASFV infection of Vero cells, protein expression was analyzed at different postinfection times (2, 4, 6, 8, 12, 24 and 48 h). Equal amount of protein from different infected cell extracts were electrophoresed and then transferred to nitrocellulose membranes and probed with antibodies against β-tubulin, viral p54, Bim and DLC8. No significant changes in Bim or DLC8 expression were found during infection (Fig. 4B).

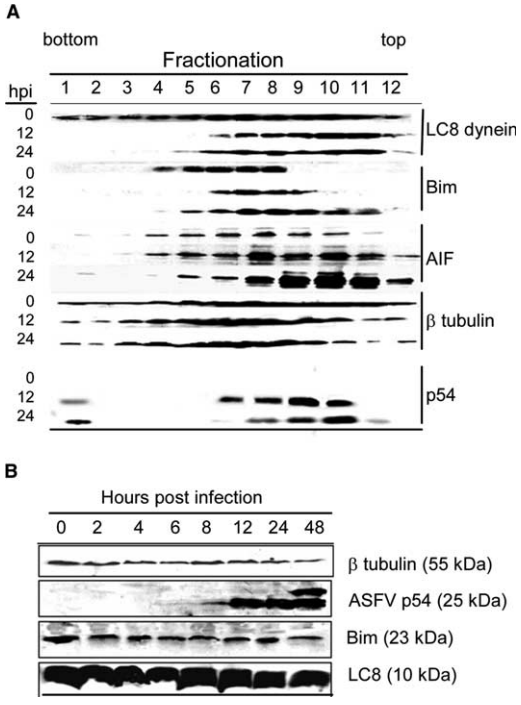

Fig. 4. Release of Bim from its sequestration site linked to microtubules after ASFV infection of Vero cells. (A) Bim translocation to soluble fractions determined by zonal sedimentation in a sucrose gradient at different hpi. Fractions were analyzed by Western blot probed with specific monoclonal antibodies to β-tubulin, Bim and AIF, rabbit antibodies against dynein (DLC8) and viral p54. (B) Western blot analysis with specific antisera against β-tubulin, viral p54, Bim and DLC8 in whole cell extracts.

4. Discussion

Apoptosis is known to play a central role in ASF pathogenesis as the virus induces cell death both in the target cell and immune defense cells [3]. ASFV infection causes caspase-9 and -3 activation followed by nuclear fragmentation characteristic of apoptosis in infected cells. Transiently expressed p54 viral protein of ASFV is able to induce apoptosis, while a mutant protein lacking the 13 aa region including the dynein-binding site did not produce activation of caspases or apoptosis. The conclusion is that p54 plays a pivotal role in ASFV-induced apoptosis.

Several structural viral proteins have been reported to induce apoptosis by interaction with the target cell in an early step of the infective cycle and in the absence of virus replication [7–10,20–22], but the mechanism underlying this induction in these viral models is to our knowledge still unknown. The apoptotic signal in ASFV is triggered without virus replication and before early protein synthesis in a postbinding step [6]. It was ruled out that the induction of apoptosis is due to the interaction of virus components with a cellular protein in the plasma membrane, as it occurs with Env protein of avian leucosis virus [21] or bovine herpes virus1 infection [22] because UV-inactivated ASFV does not induce caspase activation or apoptosis [6]. P54 plays a role in the attachment of the virion to the host cell but in neutralization experiments with monospecific and polyclonal antibodies, a remaining non-neutralized virus fraction is frequently detected [23], explaining the fact that ASFV preincubated with anti-p54 serum is still able to induce caspase-3 activation. Also, using lysosomotropic drugs it was shown that proper uncoating of ASFV particles is necessary to induce the apoptotic signal in infected cells [6]. Therefore, previous reports have shown that apoptosis

initiation could be triggered in an early infection step after receptor binding and uncoating, and these results are consistent with a role for the early intracellular transport of the virus mediated by p54.

ASFV p54 dynein-binding motif is similar to the DLC8-binding motif of Bim [1], so we investigated Bim status in ASFV infected cells. Subcellular localization of BH3 only proteins plays a critical role in cell death control, enabling the cell to react rapidly and efficiently to death signals. Bim and Bmf are held inactive by their localization to distinct cytoskeletal structures [24,25], specifically Bim is linked to the microtubular complex through DLC8 binding [24]. Single aa substitutions in Bim_L, that disrupt its interaction with DLC8, increased its killing potency to that of Bim_S [24,26], and this molecule has been considered a physiological regulator of Bim proapoptotic activity.

ASFV infection produced Bim translocation from microtubules to mitochondria. This translocation event was accompanied by initiation of downstream apoptotic events, including caspase-9 and -3 activation and alteration of nuclear and mitochondrial morphology. Further studies to address p54–dynein interaction could suggest possible links between microtubular motors and signalling pathways involved in apoptosis regulation by viruses.

In this study, we provide evidence for apoptosis induction by the mitochondrial pathway following ASFV infection and we show that ASFV p54 protein is specifically involved in this induction, although several aspects of ASFV-induced apoptosis remain unclear and further studies will be needed to gain insights into the pathways involved.

Acknowledgements: We thank Diego Megias from Universidad Autónoma de Madrid and Alberto Alvarez-Barrientos from Centro de Investigaciones Cardiovasculares for confocal microscopy assistance. This work was supported by Plan Nacional BMC2000-1003, AGL2002-00668 and European Union QLK3-2000-00362.

References

[1] Alonso, C., Miskin, J., Hernáez, B., Fernandez-Zapatero, P., Soto, L., Cantó, C., Rodríguez-Crespo, I., Dixon, L. and Escribano, J.M. (2001) African swine fever viral protein p54 interacts with the microtubular motor complex through direct binding to light chain dynein. J. Virol. 75, 9819–9827.

[2] Dixon, L.K., Costa, J.V., Escribano, J.M., Rock, D.L., Vinuela, E. and Wilkinson, P.J. (2000) *Asfarviridae*. in: Seventh Report of the International Committee on Taxonomy of Viruses (M.V.R. et al., Eds), pp. 159–165, Academic Press, New York, NY.

[3] Ramiro-Ibañez, F., Ortega, A., Brun, A., Escribano, J.M. and Alonso, C. (1996) Apoptosis: a mechanism of cell killing and lymphoid organ impairment during acute African swine fever virus infection. J. Gen. Virol. 77, 2209–2219.

[4] Cuconati, A. and White, E. (2002) Viral homologs of bcl-2: role of apoptosis in the regulation of virus infection. Genes. Dev. 16, 2465–2478.

[5] Brun, A., Rodriguez, F., Escribano, J.M. and Alonso, C. (1998) Functionality and cell anchorage dependence in insect cells of the African swine fever virus gene A179L, a viral bcl-2 homolog. J. Virol. 72, 10227–10233.

[6] Carrascosa, A.L., Bustos, M.J., Nogal, M.L., Gonzalez de Buitrago, G. and Revilla, Y. (2002) Apoptosis induced in an early step of African swine fever virus entry into Vero cells does not require virus replication. Virology 294, 372–382.

[7] Mortola, E., Noad, R. and Roy, P. (2004) Bluetongue virus outer capsid proteins are sufficient to trigger apoptosis in mammalian cells. J. Virol. 78, 2875–2883.

[8] Jan, J.T. and Griffin, D.E. (1999) Induction of apoptosis by Sindbis virus occurs at cell entry and does not require virus replication. J. Virol. 73, 10296–10302.

[9] Ramsey-Ewing, A. and Moss, B. (1998) Apoptosis induced by a postbinding step of vaccinia virus entry into Chinese hamster ovary cells. Virology 242, 138–149.

[10] Tyler, K.L., Squier, M.K., Rodgers, S.E., Schneider, B.E., Oberhaus, S.M., Grdina, T.A., Cohen, J.J. and Dermody, T.S. (1995) Differences in the capacity of reovirus strains to induce apoptosis are determined by the viral attachment protein sigma 1. J. Virol. 69, 6972–6979.

[11] King, S. (2000) The dynein microtubule motor. Biochim. Biophys. Acta 1496, 60–75.

[12] Fan, J., Zhang, Q., Tocio, H., Li, M. and Zhang, M. (2001) Structural basis of diverse sequence-dependent target recognition by the 8 kDa dynein light chain. J. Mol. Biol. 306, 97–108.

[13] Martínez Moreno, M., Navarro-Lerida, I., Roncal, F., Albar, J.P., Alonso, C., Gavilanes, F. and Rodríguez-Crespo, I. (2003) Recognition of novel viral sequences that associate to dynein light chain LC8 identified through a pepscan technique. FEBS Lett. 544, 262–267.

[14] Lo, K.W., Naisbitt, S., Fan, J.S., Sheng, M. and Zhang, M. (2001) The 8-kDa dynein light chain binds to its targets via a conserved (K/R)XTQT motif. J. Biol. Chem. 276, 14059–14066.

[15] Rodriguez-Crespo, I., Yelamos, B., Roncal, F., Albar, J.P., Ortiz de Montellano, P.R. and Gavilanes, F. (2001) Identification of novel cellular proteins that bind to the LC8 dynein light chain using a pepscan technique. FEBS Lett. 503, 135–141.

[16] Huang, D.C. and Strasser, A. (2000) BH3-Only proteins – essential initiators of apoptotic cell death. Cell 103, 839–842.

[17] Rodriguez, F., Ley, V., Gomez-Puertas, P., Garcia, R., Rodriguez, J.R. and Escribano, J.M. (1996) The structural protein p54 is essential for African swine fever virus viability. Virus Res. 40, 161–167.

[18] Gomez-Puertas, P., Rodriguez, F., Oviedo, J.M., Brun, A., Alonso, C. and Escribano, J.M. (1998) The African swine fever virus proteins p54 and p30 are involved in two distinct steps of virus attachment and both contribute to the antibody-mediated protective inmune response. Virology 243, 461–471.

[19] Gómez-Puertas, P., Rodríguez, F., Oviedo, J.M., Ramiro-Ibáñez, F., Ruiz-Gonzalvo, F., Alonso, C. and Escribano, J.M. (1996) Neutralizing antibodies to different proteins of African swine fever virus inhibit both virus attachment and internalization. J. Virol. 70, 5689–5694.

[20] Connolly, J.L. and Dermody, T.S. (2002) Virion disassembly is required for apoptosis induction by reovirus. J. Virol. 76, 6692–6696.

[21] Brojatsch, J., Naughton, J., Rolls, M.M., Zingler, K. and Young, J.A.T. (1996) CAR1, a TNF-related protein, is a cellular receptor for cytopathic avian leukosis-sarcoma viruses and mediates apoptosis. Cell 87, 845–855.

[22] Hanon, E., Meyer, G., Vanderplasschen, A., Dessy-Doizé, C., Thiry, E. and Pastoret, P.-P. (1998) Attachment but not penetration of bovine herpesvirus 1 is necessary to induce apoptosis in target cells. J. Virol. 72, 7638–7641.

[23] Gómez-Puertas, P. and Escribano, J.M. (1997) Blocking antibodies inhibit complete African swine fever virus neutralization. Virus Res. 49, 115–122.

[24] Puthalakath, H., Huang, D.C.S., O'Reilly, L.A., King, S.M. and Strasser, A. (1999) The proapoptotic activity of the bcl-2 family member Bim is regulated by interaction with the dynein motor complex. Mol. Cell 3, 287–296.

[25] Puthalakath, H., Villunger, A., O'Reilly, L.A., Beaumont, J.G., Coultas, L., Cheney, R.E., Huang, D.C. and Strasser, A. (2001) Bmf: a proapoptotic BH3-only protein regulated by interaction with the myosin V actin motor complex, activated by anoikis. Science 293, 1829–1832.

[26] Liang, J., Jafrey, S.R., Guo, W., Snyder, S.H. and Clardy, J. (1999) Structure of the PIN/LC8 dimer with a bound peptide. Nat. Struct. Biol. 6, 735–740.